# Nonlinear atomic vibrations and structural phase transitions in strained carbon chains

G.M. Chechin* and D.A. Sizintsev, O.A. Usoltsev
*South Federal University, Department of physics, Russia*
(Dated: January 18, 2017)

We consider longitudinal nonlinear atomic vibrations in uniformly strained carbon chains with the cumulene structure $(=C=C=)_n$. With the aid of ab initio simulations, based on the density functional theory, we have revealed the phenomenon of the $\pi$-mode softening in a certain range of its amplitude for the strain above the critical value $\eta_c \approx 11\,\%$. Condensation of this soft mode induces the structural transformation of the carbon chain with doubling of its unit cell. This is the Peierls phase transition in the strained cumulene, which was previously revealed in [Nano Lett. **14**, 4224 (2014)]. The Peierls transition leads to appearance of the energy gap in the electron spectrum of the strained carbyne, and this material transforms from the conducting state to semiconducting or insulating states. The authors of the above paper emphasize that such phenomenon can be used for construction of various nanodevices. The $\pi$-mode softening occurs because the old equilibrium positions (EQPs), around which carbon atoms vibrate at small strains, lose their stability and these atoms begin to vibrate in the new potential wells located near old EQPs. We introduced the simple classical model representing a chain whose particles interact via the Lennard-Jones potential that allows us to describe quite well properties of the $\pi$-mode softening. Using this model without any adjustable parameters, we were able to obtain the value of the critical strain $\eta_c$, which coincides with that found by the ab initio calculations within their accuracy. We also study the stability of the new EQPs, as well as stability of vibrations in their vicinity. In previous paper [Physica **D203**, 121(2005)], we proved that only three symmetry-determined Rosenberg nonlinear normal modes can exist in monoatomic chains with arbitrary interparticle interactions. They are the above-discussed $\pi$-mode and two other modes, which we call $\sigma$-mode and $\tau$-mode. These modes correspond to the multiplication of the unit cell of the vibrational state by two, three or four times compared to that of the equilibrium state. We study properties of $\pi$-, $\sigma$- and $\tau$-modes in the chain model with arbitrary pair potential of interparticle interactions and prove that the critical value $\eta_c$ corresponds to the inflection point of this pair potential. The similar study in the framework of the ab initio approach is difficult by necessity to have a sufficiently acceptable description of the van der Waals interactions for atomic vibrations with large amplitudes. The analysis of the possible condensation of $\sigma$- and $\tau$-modes allows us to suppose that two new types of carbon chains (besides cumulene and polyyne) can exist with bond lengths alternation different from that of polyyne.

PACS numbers: 81.05.U-, 63.20.Ry, 63.20.dk, 64.60.A-

arXiv:1701.04543v1 [nlin.PS] 17 Jan 2017

## I. INTRODUCTION

Monoatomic carbon chains can exist in two different modifications. The first one is polyyne, or carbyne-$\alpha$, representing the chain with alternating single and triple bonds [chemical structure $(-C \equiv C-)_n$]. The second modification is cumulene, or carbyne-$\beta$, representing the chain with double bonds [chemical structure $(=C=C=)_n$]. Carbyne chains was claimed to be the strongest material known at the present time. The synthesis of linear carbon chains up to 6000 atoms was reported in 2016. Because of many unique mechanical, physical and chemical properties, which were studied or only predicted, carbyne is considered as perspective material for various nanodevices, for hydrogen storage, etc. (see [1–5] and papers cited therein).

Chemical synthesis of pure carbyne chains and their experimental study are very difficult and, therefore, theoretical ab initio investigations, in particular those based on the density functional theory (DFT), play a rather important role for prediction of its properties and for treating different physical phenomena, which are possible in this material. Many interesting results on strained carbyne chains were obtained with DFT computer simulations. In the paper [5], DFT *ab initio* methods allow to reveal that distribution of bond length and magnetic moments at atomic sites exhibit even-odd disparity depending on the number of carbon atoms in the chain and on the type of saturation of these atoms at both ends. It was also found that a local perturbation created by a small displacement of the single carbon atom at the center of a long chain induces oscillations of atomic forces and charge density, which are carried to long distances over the chain.

In the paper [1], the structural transformation of cumulene under a certain strain was revealed. This is the Peierls phase transition, which leads to the radical change of carbyne electron spectrum. As a result of this transition, an energy gap in the electron spectrum appears and the conductive cumulene transforms into polyyne which is semiconductor or insulator. This phenomenon opens perspectives to control electrical behavior of carbyne by mechanical strain [1].

During the study of different types of nonlinear atomic

* gchechin@gmail.com

vibrations in strained cumulene chains, under periodic boundary conditions, we revealed an unexpected phenomenon of softening of the longitudinal $\pi$-mode vibrations above a certain critical value of the strain. Some results of this study were published in the brief paper [6]. They can be summarized as follows[1].

For strains lower than $\eta = 11\,\%$ cumulene demonstrates monotonic *hard* type of nonlinearity (the frequency increases with increasing the $\pi$-mode amplitude $a$). However, for $\eta > 11\,\%$ there is a certain range of amplitudes $a$ in which *soft* nonlinearity occurs, namely, the frequency of the $\pi$-mode abruptly *decreases* and then again begins to increase.

The phenomenon of vibrational modes softening is well known in the theory of structural phase transitions [7] where by condensation ("freezing") of such modes one tries to explain the nature of the displacement-type phase transitions. This is the so-called concept of *soft modes*. It is essential that in the majority of the papers on this subject, soft modes are treated in purely phenomenological manner with some vague arguments about changing of electron-phonon interactions in crystal under change of such external parameters as temperature and pressure. Unlike these works, in our study a soft vibrational mode in cumulene appears as a direct result of the ab initio simulation *without* any additional assumptions.

In [6], the phenomenon of the $\pi$-mode softening has been explained by the fact that above the critical value of the strain the old atomic equilibrium positions (EQPs) become unstable and two new EQPs appear near each of them. Namely, vibrations in the vicinity of these new EQPs correspond to the softening of the $\pi$-mode. In turn, condensation of the $\pi$-mode leads to a new atomic equilibrium configuration that corresponds to the Peierls phase transition. After this transition, the unit cell turns out to be twice as large than that of cumulene, and the carbon chain transforms into another carbyne form, polyyne, with bond lengths alternation.

The main ab initio results obtained in our work and in the paper [1] are sufficiently close to each other. Some discrepancy can be explained by different approximations used in the framework of DFT approach (different exchange-correlation functionals, different sets of basis functions for solving Kohn-Sham equations, different realization of the numerical methods in the packages ABINIT and VASP, etc.). Nevertheless, our results and those from [1] are identical qualitatively (detailed comparison will be presented elsewhere).

In the present paper, we discuss in detail the condensation of the $\pi$-mode as well as the condensation of two other symmetry-determined nonlinear normal modes, which are possible in cumulene chains. With the aid of our approach combined with some group-theoretical methods [8], we predict the possibility of existence of two new types of carbon chains, besides cumulene and polyyne. They both possess alternation of bond lengths, but with *different alternating schemes* compared to that of the polyyne.

This paper is organized as follows. In Sec. II, we consider the $\pi$-mode atomic vibrations in the strained cumulene in the framework of the DFT model and discuss the properties of these vibrations near new EQPs. The simple model of the monoatomic chain whose particle interact via the Lennard-Jones potential (L-J chain) is introduced in Sec. III and the appearance of the new EQPs is explained. In Sec. IV, we discuss the stability of these equilibrium positions. In Sec. V, the notion of the symmetry-determined Rosenberg NNMs in monoatomic chains is considered. In Sec. VI, we discuss the properties of these modes in the framework of the L-J model and results of their condensation in the cumulene chains. Sec. VII contains some conclusion remarks on nonlinear dynamics of the strained carbon chains.

## II. $\pi$-MODE VIBRATIONS WITHIN DFT MODEL

We investigate *longitudinal* atomic vibrations of *uniformly strained* carbon chains in the $\pi$-mode dynamical regime. This strain is modeled by an artificial increase of the unit cell size ($R$) with respect to that of the chain without strain ($R_0$). Thus, speaking about the strain of the chain by $\eta$ per cent, we mean that $R = R_0\,(1+\eta)$.

The set of atomic displacements $\boldsymbol{X}\,(t) = [x_1\,(t)\,,\, x_2\,(t) \ldots x_N(t)]$ of the $N$-particle carbon chain for such vibrational regime at a fixed time $t = t_0$ can be written as follows:

$$\boldsymbol{X}(t_0) = [a(t_0), -a(t_0)\,|a\,(t_0)\,, -a(t_0)| \ldots$$

$$\ldots |a(t_0), -a(t_0)]. \qquad (1)$$

In this pattern, all $x_i\,(t)$ with odd numbers are equal to $a\,(t_0)$, while those with even numbers are equal to $-a\,(t_0)$. Thus, all neighboring atoms vibrate out of phase with equal amplitudes. The unit cell for describing $\pi$-mode vibrations of the chain with periodic boundary conditions is twice larger than that of the equilibrium state. Since two carbon atoms in this unit cell possess, at any time $t$, displacements $x(t)$ and $-x(t)$, one can discuss the time evolution of only one of them choosing the origin at its equilibrium position. To excite the $\pi$-mode vibrations in the chain we assume $x(0) = a$, $\dot{x}(0) = 0$.

The $\pi$-mode *nonlinear* oscillations in the strained cumulene we study with the aid of DFT theory [9] using for this propose the software package ABINIT [10, 11].

The Born-Oppenheimer approximation was used to separate fast motion of electrons and slow motion of nuclei. At each time step for fixed positions of nuclei, self-consistent electron density distribution is calculated

[1] Unfortunately, we were not aware of the paper [1] when prepared our own paper [6].

by solving Kohn-Sham quantum-mechanical equations. Then forces acting on the nuclei are computed, and their new configuration is found by using one step of solution of classical dynamical equations. For this new configuration, the procedure of self-consistency for the electron subsystem is repeated.

All calculations are performed in the framework of the local density approximation (LDA). Pseudo-potentials by Troullier-Martins was used to describe the field of the carbon atoms inner shells in the process of the Kohn-Sham equations solving with the aid of the plane waves basis (energy cutoff is equal to 1360 eV). The convergence for energy is chosen as $10^{-8}$ eV between two steps.

Hereafter, considering ab initio simulations, we speak about the study of nonlinear oscillations in the framework of the *DFT model* emphasizing that our calculations provide only an approximation to the real physical picture.

An important feature of nonlinear vibrations is the dependence $\omega(a)$ of the frequency ($\omega$) on the amplitude ($a$). To find this dependence, we carried out a series of *ab initio* calculations. For each computational run, with fixed values of the strain and the amplitude (parameter) $a$ of the $\pi$-mode, the frequency $\omega(a)$ was calculated. In Fig. 1, we present the function $\omega(a)$ for chains with 5 %, 7,5 % and 10 % strain. This figure demonstrates that *hard type of nonlinearity* appears at relatively small strains (increase of amplitude results in increase of frequency).

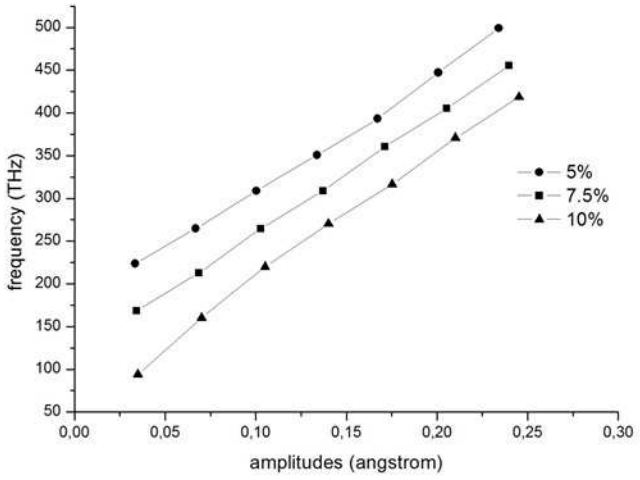


FIG. 1. Dependence of the frequency ($\omega$) of the $\pi$-mode on its amplitude ($a$) for small strains of the carbyne chain.

However, we have revealed unexpected behavior of the function $\omega(a)$ for the strain above the critical value $\eta_c = 11\,\%$. For example, one can see in Fig. 2 that this function for $\eta = 15\,\%$ turns out to be nonmonotonic and *softening* of the $\pi$-mode, at a certain interval of the parameter ($a$), takes place.

It is essential that for the $\pi$-mode parameter $a$ belonging to the interval [**A**, **B**] (Fig 2) the carbon atom oscillates about a *new equilibrium position* different from the old one at $x = 0$. This effect is illustrated in Fig. 3

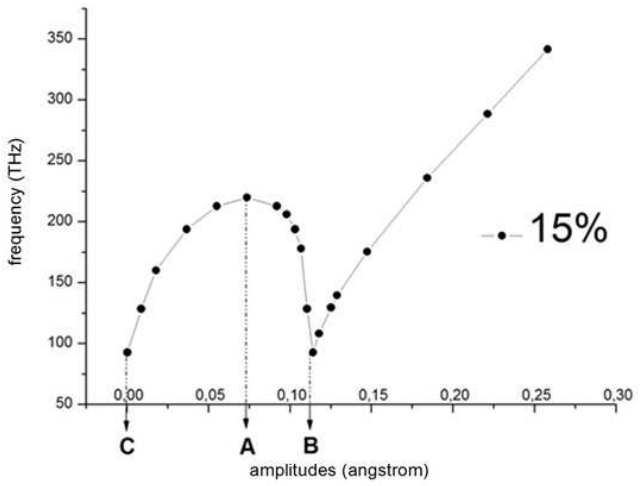


FIG. 2. Dependence of the frequency ($\omega$) of the $\pi$-mode on its amplitude ($a$) for 15 % strain of the carbyne chain.

for the chain strained by 15 % (detail discussion of these oscillations is given below in Sec. IV).

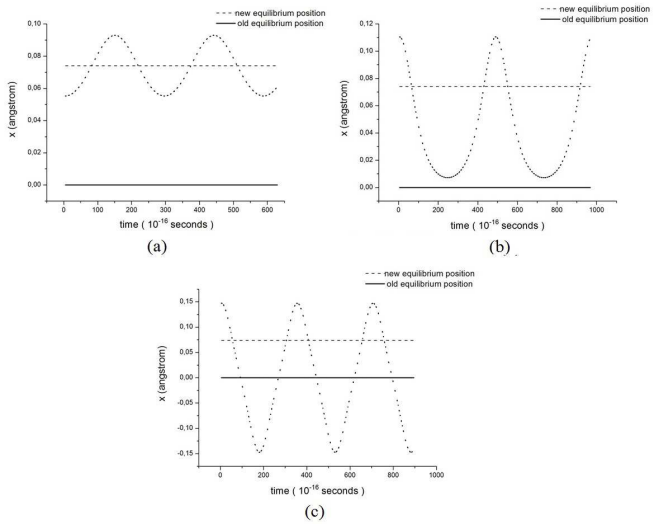


FIG. 3. Oscillations of the carbon atom for different $\pi$-mode amplitudes: (a) oscillations in the small potential well near the new equilibrium position; (b) oscillations before the escape from the small potential well; (c) oscillations in the large potential well with respect to the old equilibrium position.

To explain the above behavior of the function $\omega(a)$ one can study the potential energy[2] of the $\pi$-mode $U(a)$ as a function of its parameter $a$ for different strains of the carbon chain. For this purpose, we fix the configuration of

[2] We excite the $\pi$-mode vibrations by assigning to all carbon atoms the same displacements ($a$) and zero velocities at initial time. Thus, the total energy $E(a)$ of the carbyne chain at this instant is equal to its potential energy $U(a)$.

carbon nuclei choosing a concrete value of the parameter $a$, and then find the potential energy $U(a)$ of this configuration with the aid of the software package ABINIT.

The energy profiles $U(a)$ for different strains of carbon chains are shown in Fig. 4. From this figure, one can see that with increase of the strain, the energy profiles $U(a)$ become flatter near the origin ($a = 0$) and their curvature changes sign after passing through zero. As a result, the *old* equilibrium position ($a = 0$) becomes unstable, and two *new* minima appear at equal distances on both sides of the origin. This specific behavior of potential energy of strained carbon chains helps us to explain the properties of the amplitude-frequency dependence $\omega(a)$ shown in Fig. 2. Let us consider this question in more detail.

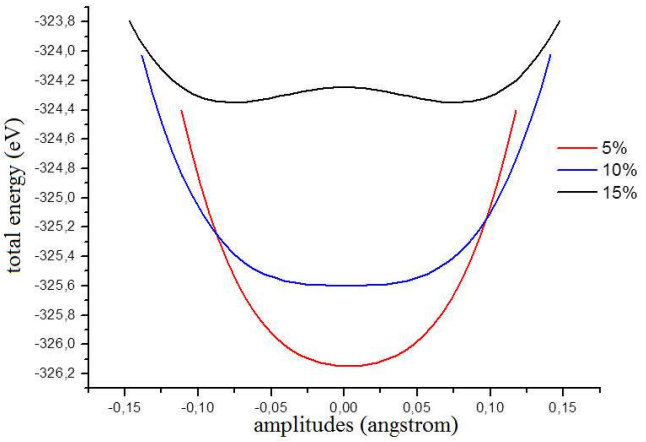


FIG. 4. Profiles of the potential energy of cumulene chains for different strains (color online).

In Fig. 5, one can see the $\pi$-mode potential energy profile for the strain $\eta = 15\,\%$, as well as some fitting of this profile in the framework of the Lennard-Jones model, which is discussed in the next section. The points A and B ($B'$) in this figure correspond to the old and new equilibrium positions, respectively.

Next, we study the atomic vibrations in the potential wells depicted in Figs. 5 and 6.

Let us consider the $\pi$-mode energy $E_0 = u(a_0)$ that corresponds to the new equilibrium position $a = a_0$, i.e. to the bottom B of the right potential well in Fig. 5. The frequency $\omega(a)$ of the atomic oscillations near the point $B$ (for example, between returning points $d$ and $d'$ in Fig. 6) *decreases* with increasing of the energy $E$ from $E_0$ up to the value $E_c$ which is determined by the top of the potential hill at $a = 0$. Thus vibrations in the "small" potential well demonstrate the *soft* type of nonlinearity.

There is a certain gap in the function $\omega(a)$ for further increase of $E$, because the carbon atom begin to oscillate in the "large" potential well (for example, between points $e$ and $e'$ in Fig. 6) around the *old* equilibrium position at $a = 0$. The increasing of the energy E of the $\pi$-mode in this well leads to increasing of the frequency $\omega(a)$. Such behavior of the frequency corresponds to the *hard* type of nonlinearity.

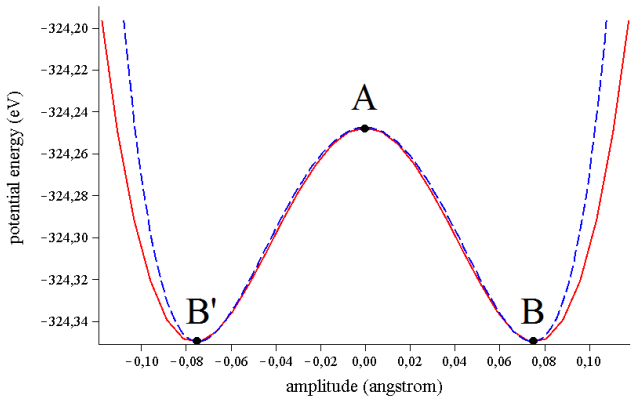


FIG. 5. The $\pi$-mode energy profile for the strain $\eta = 15\,\%$. The points A and B ($B'$) correspond to the old and new equilibrium positions of carbon atom, respectively. The solid curve shows the ab initio results, while the appropriate fitting in the framework of the Lennard-Jones model is shown by the dashed curve.

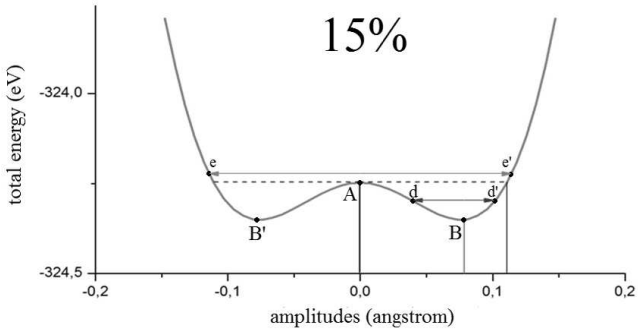


FIG. 6. The potential energy profile of the carbyne chain under 15 % strain and the $\pi$-mode oscillations of carbon atom with respect to the new (point B) and old (point A) equilibrium positions.

Thus, the phenomenon of the $\pi$-mode softening can be explained by the atomic vibrations near the new equilibrium positions in small potential wells of the strained chain. This phenomenon will be considered in more detail in the framework of the Lennard-Jones model in the next section.

Comparing the above described behavior of the frequency $\omega(a)$ with that depicted in Fig. 2, one has to take into account that the amplitude of the atomic oscillations near the old equilibrium positions at $a = 0$ coincides with the $\pi$-mode parameter $a$, while the vibrational amplitude in the small potential well near new equilibrium positions is equal to $(a - a_0)$. This is the reason why we prefer to call $a$ by the term "$\pi$-mode parameter" rather than "$\pi$-mode amplitude".

The condensation of the $\pi$-mode leads to appearance of two domains of the structural phase transition of the displacement type. If all carbon atoms of the chain are located in the right potential wells, we have one domain,

while another domain corresponds to the localization of the atoms in the left wells. In both domains, there is a bond length alternation (BLA) which can be seen in Fig. 7, where $l_1 = l_0 - a_0$ and $l_2 = l_0 + a_0$ are short and long interparticle distances (bond length) for $a_0 > 0$ and vice versa for $a_0 < 0$. From Fig. 7, we find the following BLA for the $\pi$-mode condensation:

$\mathrm{BLA}_\pi = [l_1,\ l_2|l_1,\ l_2|...|l_1,\ l_2]$.

This BLA corresponds to the polyyne structure of the carbon chain.

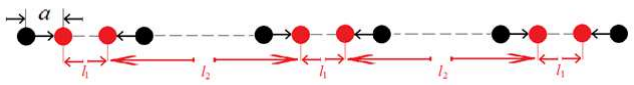


FIG. 7. Bond lengths alternation in strained carbyne for the pattern (1) with $a(t_0) = a$. Here, for $a > 0$ values $l_1$ and $l_2$ are short and long bonds, respectively, and vice versa for $a < 0$ (color online).

The transformation from cumulenne to polyyne structure can be observed as a result of the appropriate increasing of the magnitude $\eta$ of the strain above the critical value $\eta_c$ when the old equilibrium positions lose stability and two new ones appear near each of them. In Fig. 8, we present the dependence $a_0(\eta)$ of the position $a_0$ of the new equilibrium state on the strain $\eta$. The bifurcation takes place approximately at $\eta_c = 11\,\%$.

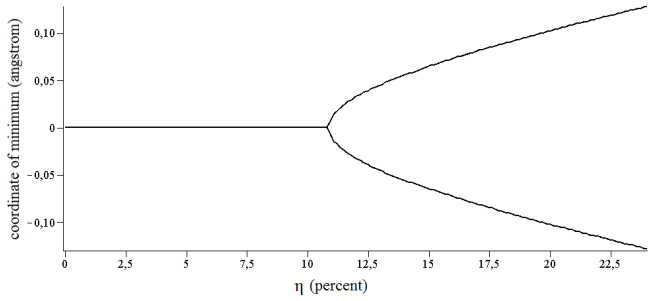


FIG. 8. Dependence of the $\pi$-mode parameter $a_0$ on the strain $\eta$, which corresponds to the minimum of the potential energy (point B in Fig. 5.).

## III. THE LENNARD-JONES MODEL

Now we consider the Lennard-Jones model, which is associated with the molecular dynamics approach. The main idea of the molecular dynamics can be formulated as follows. Molecules (atoms) are replaced by mass points whose interactions are described with the aid of some phenomenological potentials. For the obtained dynamical system, equations of classical mechanics are solved. In the framework of quantum mechanics, such approach cannot be considered as sufficiently adequate, because it is difficult or impossible to find potentials which are good enough to take into account the influence of atomic electron shells on dynamical properties of the original physical system. That is why one has to use very complicated many-particle potentials which possess different forms for different geometry of the interacting atoms and contain phenomenological constants defined by huge tables (see, for example, [12]).

However, in some cases, reasonable results can be obtained even with the aid of simple pair potentials, such as those by Morse, Lennard-Jones, etc. For example, one can refer to the paper [13] devoted to study discrete breathers in 2D and 3D Morse crystals. Below, we try to explain the above-discussed results, obtained by *ab initio* calculations for the $\pi$-mode dynamics in carbyne, using the model of a chain whose particles interact via the Lennard-Jones potential (L-J chain).

Let us remind some well-known properties of this potential which can be written in the form

$$\varphi(r) = \frac{A}{r^{12}} - \frac{B}{r^6}. \qquad (2)$$

Here the first term describes repulsion between two particles that are at distance r from each other, while the second term describes their attraction. The space dependence of this attraction can be explained in the framework of quantum mechanics as a result of the induced dipole-dipole (van der Waals) interaction, while the 12-th degree of the distance r in repulsive term of Eq.(2) is introduced only for computational convenience. An important feature of the Lennard-Jones potential is that its both constants, A and B, can be chosen equal to unity ($A = B = 1$) without loss of generality, if we make an appropriate scaling of space and time variables in dynamical equations constructed with the aid of this potential.

The dependence of the $\pi$-mode energy on the parameter $a$ was shown in Fig. 5, where the solid line corresponds to the results of *ab initio* calculations, while the dashed line is used for the L-J model. We use the simplest fitting for the energy profile corresponding to the L-J model. It was obtained by such choice of two Lennard-Jones parameters, A and B from Eq.(2), that the energy at the points A and B (see Fig. 5) coincides with the energy of the profile found by *ab initio* calculations. Note that Fig.5 corresponds to the strain $\eta = 15\,\%$ and for this case $a_0$ is equal to 0,075$\mathring{A}$.

In Fig.5, one can see considerable discrepancy between

the energy profile u($a$), which was found by ab initio calculations and its Lennard-Jones fitting in the case of large values of the $\pi$–mode parameter $a$. The fitting based on the Morse potential is slightly better, but the above discrepancy also turns out to be considerable. Certainly, one can set a goal to find such pair potential that provides more satisfactory fitting, but this goal is not too important. The matter is that the function u($a$), in the framework of the ABINIT model, can be found only with low accuracy for large values of the $\pi$–mode parameter $a$. Indeed, such values correspond to large amplitudes of atomic vibrations and one has to apply a rather accurate expression for the van der Waals interactions. On the other hand, these interactions are essentially nonlocal and cannot be described correctly in the framework of the conventional DFT theory, at least with the aid of the approximations used in such software packages as ABINIT, VASP, etc.. We discuss this problem in the last section of the present paper.

We verified that dynamical properties of the $\pi$-mode obtained by the *ab initio* study (see Fig. 2) and those obtained by molecular dynamics for the L-J chain are in qualitative agreement. The above facts seem to be important since computer experiments, based on the density functional theory, require very long time in contrast to those based on the methods of molecular dynamics. Therefore, one can use the L-J chain modeling to predict some dynamical properties of the carbyne, which then may be verified by *ab initio* calculations.

It is very interesting to clear up the nature of evolution of the carbyne properties with increasing of the strain. Why old equilibrium positions lose their stability and new stable equilibrium positions appear? This problem can be understood with the aid of the following simple L-J model.

Let us consider a system of three carbon atoms located at a distance R from each other symmetrically about the origin $x = 0$ (see Fig. 9). Positions of the atoms 1 and 3 are fixed, while the "inner" atom 2 can be displaced by a certain value $x$ from its old equilibrium position at origin. We assume that atoms interact via the Lennard-Jones potential $\varphi(x)$ from Eq.(2) with $A = B = 1$ (hereafter, it will be called the standard L-J potential).

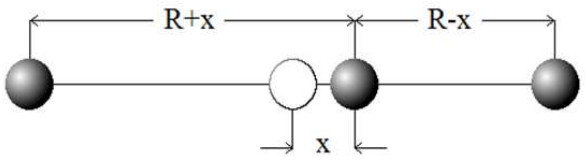


FIG. 9. Simple model of three atoms interacting via the Lennard-Jones potential. Atoms 1, 3 are fixed, while atom 2 is displaced by $x$ from its old equilibrium position at origin.

If the coordinate x corresponds to the equilibrium state of the atom #2, then the forces $f\,(r)$ acting on it from the left and right neighbors must be equal:

$$f(R+x) = f(R-x), \tag{3}$$

where

$$f(r) = -\frac{\mathrm{d}\varphi}{\mathrm{d}r} = \frac{1}{r^{12}} - \frac{1}{r^{7}}. \tag{4}$$

Eq.(3) represents a nonlinear equation with respect to x that may have *several* real roots. We depict this situation in Fig. 10 where intersection points of the functions $f(R+x)$ and $f(R-x)$ at $x = 0$ and at $x = 0{,}065$ take place. Here $R = 1{,}291$ corresponds to the 15 % strain of the carbyne chain. The root $x = 0$ is associated with old equilibrium position that becomes unstable, while the roots $x = 0{,}065$ are associated with the new ones. Thus, the cause of the appearance of the new equilibrium positions becomes obvious.

It is also easy to verify that the curvature of the potential energy of the considered system is negative for $R = 1{,}20$ (stable equilibrium), while it becomes positive for $R = 1{,}25$ (unstable equilibrium). Note that one can reveal the similar behavior of the potential energy for L-J chains with arbitrary number of atoms.

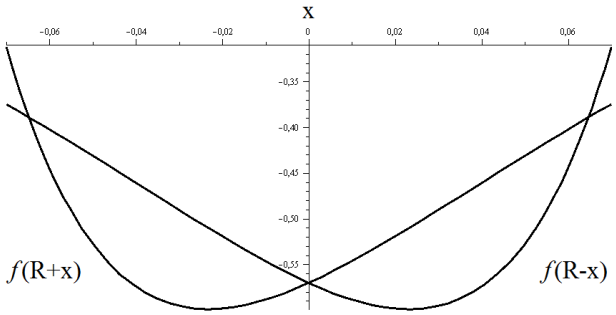


FIG. 10. Appearance of the new equilibrium positions in the simple model of three particles interacting via the Lennard-Jones potential.

It is interesting to study nonlinear atomic vibrations in the potential well corresponding to the standard L-J model (this well is similar to that depicted in Fig.6 for the ABINIT model). In Fig. 11, we show some arbitrary chosen energy levels in the small right well near the new equilibrium position, as well as levels above the potential hill which correspond to vibrations in the large potential well around the old equilibrium position ($a = 0$). The frequencies corresponding to these levels are presented in Table 1. From this table one can see the soft nonlinearity of vibrations near the new EQPs in the small right potential well (the frequency decreases with increasing of the energy) and the hard nonlinearity above potential hill in the large well (the frequency increases with increasing of the energy). Naturally, there is a certain *gap* in the frequency spectrum near the top of the potential hill. According to Table 1, this gap takes place between energy levels $E_5$ and $E_6$.

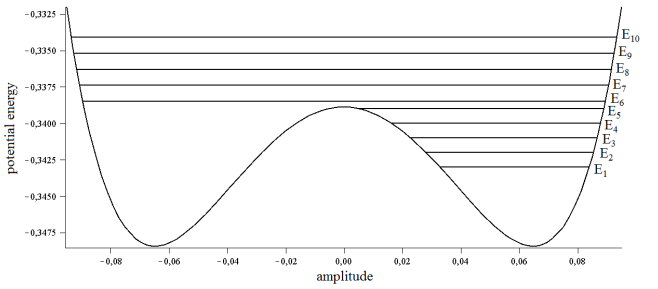


FIG. 11. Some energy levels in the potential well for the Lennard-Jones model, which correspond to the values shown in Table I.

TABLE I. Dependence of the frequency $\omega_j$ on the energy level $E_j$ for the Lennard-Jones model.

| $j$ | $E_j$ | $\omega_j$ |
|---|---|---|
| 1 | -0, 3430 | 2, 7070 |
| 2 | -0, 3430 | 2, 5711 |
| 3 | -0, 3410 | 2, 4011 |
| 4 | -0, 3400 | 2, 1610 |
| 5 | -0, 3390 | 1, 5942 |
| 6 | -0, 3385 | 0, 9243 |
| 7 | -0, 3374 | 1, 1551 |
| 8 | -0, 3363 | 1, 2867 |
| 9 | -0, 3352 | 1, 3872 |
| 10 | -0, 3341 | 1, 4710 |

## IV. STABILITY OF THE $\pi$-MODE VIBRATIONS NEAR THE NEW EQUILIBRIUM POSITIONS

In previous sections, we have solved the problem of existence of the new equilibrium positions for strained carbon chains in the framework of the DFT ab initio approach, as well as for the Lennard-Jones model. Now let us consider the problem of their stability. This problem can be formulated as follows. We must verify if a given new equilibrium position corresponds to a minimum of the potential energy $U(\boldsymbol{X})$, which is a function of $N$-dimensional vector $\boldsymbol{X} = [x_1, x_2, ..., x_N]$ of *all degrees* of freedom of our chain. Note, that the minimum in Fig.5 corresponds to the one-dimensional function $u(a)$, where $a$ is the $\pi$-mode amplitude, and the vector $\boldsymbol{X}(t) = [a, -a|a, -a|...|a, -a]$ determines the position of this minimum in the $N$-dimensional space.

For example, below we study stability of the new equilibrium positions for the carbon chain of $N = 8$ atoms. Let us again consider the point B at the bottom of the right potential well in Fig. 5. If B represents a minimum of the potential energy $U(\boldsymbol{X})$ in the full eight-dimensional space of all possible displacements, then infinitesimal shift from this point in *any direction* leads to increase of the function $U(\boldsymbol{X})$. It is well known that the local extremum of the function $U(\boldsymbol{X})$ in many-dimensional space can be of different type (minimum, maximum or a saddle point). The most effective way to analyze the type of a given extremum point $\boldsymbol{X}_0$ (it determines the equilibrium position) can be carried out for the L-J model by the following procedure.

Let us expand the function $U(\boldsymbol{X})$ near the point $\boldsymbol{X}_0$ into many-dimensional Taylor series and restrict it by quadratic terms only (this procedure corresponds to analyzing the harmonic approximation in the framework of the dynamical approach). The obtained *quadratic form* is then transformed by a certain linear transformation of variables to the *canonical* form, which represents a superposition only of squares of new variables with some coefficients $\lambda_j (j = 1..N)$. These coefficients can be found by diagonalization of the matrix of the original quadratic form as its eigenvalues. The extremum $\boldsymbol{X}_0$ will be a minimum only if $\lambda_j \geq 0$ for all $j = 1..N$. If a certain eigenvalue turns out to be negative ($\lambda_{j0} < 0$), then any infinitesimal shift by $\gamma$ from the point $\boldsymbol{X}_0$ along the line $\boldsymbol{X} = \boldsymbol{X}_0 + \gamma\boldsymbol{\xi}_{j0}$, where $\xi_{j0}$ is the eigenvector corresponding to $\lambda_{j0}$, leads to decrease of the function $U(\boldsymbol{X})$ and, therefore, $\boldsymbol{X}_0$ is a saddle point (or maximum, if all $\lambda_j \leq 0$).

With the aid of the above procedure, we have obtained for the standart L-J model the following results for the eight-particle chain under uniform strain $\eta = 15\,\% : \lambda_1 = 0$, $\lambda_2 = +88{,}4$, $\lambda_3 = \lambda_4 = +100{,}6$, $\lambda_5 = +110{,}6$, $\lambda_6 = \lambda_7 = -12{,}2$, $\lambda_8 = -22{,}2$ (these values were rounded up to 1 figures after decimal point). The obtained result is disappointing since the new EQP turns out to be a saddle point (three $\lambda_j < 0$) and, therefore, this equilibrium state is *unstable*.

Now we can analyze the energy profiles $U(\boldsymbol{X})$ along eight lines $\boldsymbol{X} = \boldsymbol{X}_0 + \gamma\boldsymbol{\xi}_{j0}$ $(j = 1..8)$ in the eight-dimensional space. Here $\gamma$ is a sufficiently small number because we want to compare the corresponding results with those obtained for energy function considered as a quadratic form. The energy profiles $U(\boldsymbol{X}) = u_j(\gamma)$ for all basis directions $\boldsymbol{\xi}_j$ are depicted in Fig. 12. We exclude the vector $\boldsymbol{\xi}_2$ from our consideration because it determines the direction along the $\pi$-mode and, therefore, it has no relation to the stability of this mode.

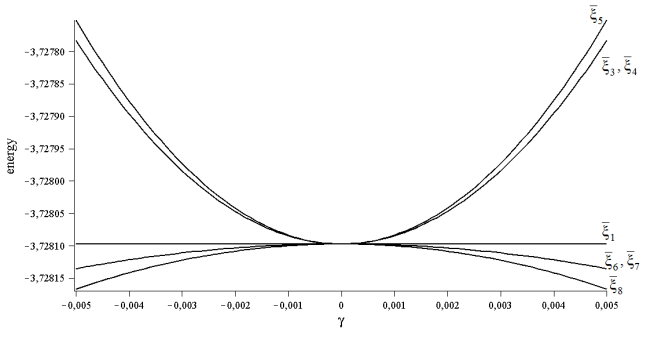


FIG. 12. Energy profiles for the L-J chain with $N = 8$ particles for all basis directions $\boldsymbol{\xi}_j$ $(j = 1..8)$ except $\boldsymbol{\xi}_2$.

The graphs from this figure fully confirm the previously discussed results on stability properties of the new equi-

librium position $\boldsymbol{X}_0$. Indeed, we see decrease of energy for $\lambda_j < 0$ ($\lambda_6 = \lambda_7$, $\lambda_8$), increase of energy for $\lambda_j > 0$ ($\lambda_3 = \lambda_4$, $\lambda_5$) and constant energy for $\lambda_1 = 0$. Thus, the new EQP in carbyne with 15 % strain, which corresponds to the vector$\boldsymbol{X}_0 = [a_0, -a_0|a_0, -a_0|a_0, -a_0|a_0, -a_0]$ with $a_0 = 0{,}075$, occurs to be unstable in the framework of the Lennard-Jones model. It can be proved that this conclusion is true for arbitrary number $N$ of particles in the L-J chain.

The above described method can be easily applied to the study of stability properties of new equilibrium positions in strained carbyne in the framework of the ab initio DFT approach. In Fig. 13, we present potential energy profiles calculated by ABINIT software package [10, 11] for 15 % strained cumulene chain of $N = 8$ atoms for the above discussed basis directions.

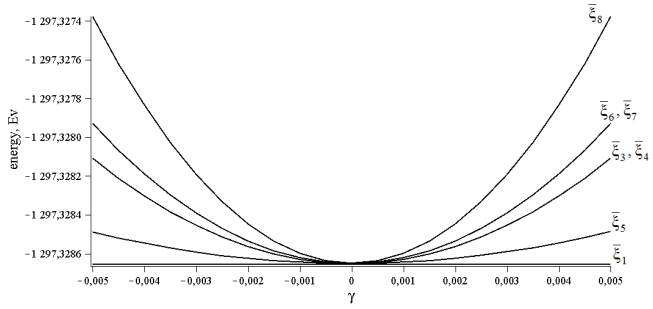


FIG. 13. Energy profiles for the carbyne chain of $N = 8$ particles for basis directions $\xi_j$, which are obtained in the framework of the *ab initio* DFT model.

The obtained results turn out to be unexpected, because the energy profiles in Fig. 13, unlike those in Fig. 12, demonstrate *minima* for all basis directions.Thus, the new equilibrium position, at point B in Fig. 5, being unstable in the L-J model, occurs to be *stable* in the framework of the DFT model. Why such discrepancy does take place? We discuss this issue in the last section of the present paper.

Let us now consider the problem of stability of atomic *vibrations* near the new equilibrium positions in strained carbon chains. In Fig. 14, we represent for $\eta = 15\,\%$ strain the time-evolution of the carbon atom oscillations in the right potential well (see Fig. 5) approximately at the middle of its depth. The dashed line corresponds to the DFT model, while the dotted line demonstrates oscillations for the L-J model.

To analyze the stability of these oscillations we add to the initial $\pi$-mode profile

$$\boldsymbol{X}(0) = [a(0), -a(0)|a(0), -a(0)|a(0), -a(0)a(0), -a(0)],$$

$$a(0) = 0,\,075 \qquad (5)$$

a small perturbation in the form $\gamma\boldsymbol{\xi}_8$ with $\gamma = 10^{-3}$, where $\boldsymbol{\xi}_8$ is the basis vector, which corresponds to the

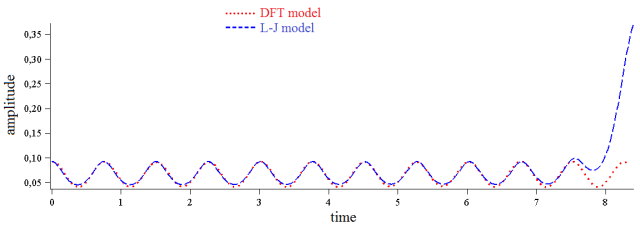


FIG. 14. Time-evolution of the $\pi$-mode initial profile (5) in DFT and L-J models for the eight-particle carbyne chain under 15 % strain.

negative eigenvalue with maximal absolute value ($\lambda_8 = 22{,}2$). It is obvious from Fig. 14 that solution of the Newton ordinary differential equations, corresponding to the L-J model, demonstrates *hard instability* (dashed line) already at ten oscillation periods ($t \approx 10T$). In contrast to this result, we have found that the DFT solution for the same initial conditions (dotted line) demonstrates a fine stability, at least up to the time interval $t \approx 100T$. The small modulation of the periodic oscillations in the DFT model is induced by the above mentioned perturbation $\gamma\boldsymbol{\xi}_8$ ($\gamma = 10^{-3}$) artificially added to exactly periodic initial $\pi$-mode profile (5).

Thus, we can conclude that the $\pi$-mode atomic vibrations in the L-J model are unstable, while they demonstrate stability in the DFT model (at least, by visual inspection). Remember, that the analogical discrepancy between static properties of the L-J model and the DFT model was discussed in the previous section.

Because of importance of this conclusion, we verify by the rigorous Floquet method that periodic atomic vibrations in the L-J chain are indeed unstable. The similar stability analysis for DFT model is yet not carried out because of some computational difficulties.

## V. ROSENBERG NONLINEAR NORMAL MODES

Nonlinear normal mode by Rosenberg (NNM) represents a periodic vibrational regime for which all degrees of freedom $x_i(t)$, at any time $t$, are proportional to each other [14, 15]. This definition can be written in the form

$$x_i(t) = a_i f(t) \quad (i = 1..N), \qquad (6)$$

where $a_i$ are constant coefficients, while $f(t)$ is the same time-dependent function for all degrees of freedom. If the explicit form of dynamical equations is known, the substitution of the ansatz (6) into these equations leads to a system of $(N-1)$ nonlinear algebraic (or transcendental) equations for coefficients $a_i$ and a single differential equation for the function $f(t)$. Note that the conventional linear normal modes represent a special case of Rosenberg modes. In this case, $f(t) = \cos(\omega t + \varphi_0)$ where $\omega$ and $\varphi_0$ are frequency and initial phase, while coefficients

$\{a_i | i = 1..N\}$ from Eq.(6) are amplitudes of the different degrees of freedom.

In contrast to the case of linear normal modes, the number of Rosenberg modes has no relation to the dimension of the system. It is essential that Rosenberg NNMs can exist only in very specific dynamical systems, in particular, in those, whose potential energy is a homogeneous function of all its arguments. On the other hand, it was shown in [8, 16] that there can be some *symmetry-related* reasons for existence of NNMs in systems with arbitrary interparticle interactions. These dynamical objects we call Rosenberg symmetry-determined nonlinear normal modes (below the specification "symmetry-determined" is omitted because we consider only such type of modes).

Let us consider $N$-particle monoatomic chain with periodic boundary conditions and arbitrary interparticle interactions. The group theoretical method for obtaining all nonlinear normal modes in such chain can be outlined as follows (see details in [8]).

All dynamical regimes in the physical system with discrete symmetry group $G_0$ in its equilibrium state can be classified by subgroups $G_j$ of this group ($G_j \subset G_0$). One can obtain the general form of the dynamical regime corresponding to the subgroup $G_j$ by solving the equation $\hat{G}_j X = X$, where the vector $X(t) = [x_1(t), x_2(t), ..., x_N(t)]$ describes displacements of all degrees of freedom $x_i(t)$ at arbitrary fixed time $t$. In other words, $X(t)$ must be an *invariant vector* of the operator group $\hat{G}_j$ acting in the $N$-dimensional space which is induced by the group $G_j$.

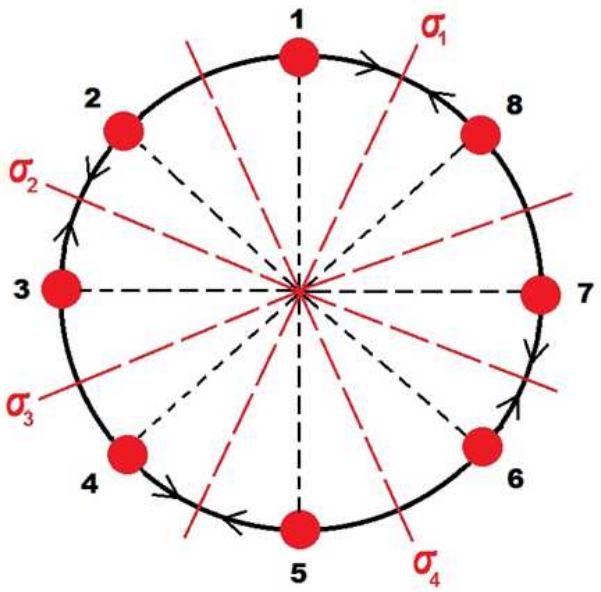


FIG. 15. Displacement pattern of the $\pi$-mode for the chain with $N = 8$ particles (color online).

This chain in the equilibrium state can be represented as a ring (see, for example, Fig. 15) with the point group $D_N$. In [8], we proved that only following three Rosenberg NNMs can exist in such chains depending on the number $N$ of their particles:

$$\pi - \text{mode: } \boldsymbol{X}(t) = [a(t), -a(t) \mid a(t), -a(t) \mid ...$$

$$... \mid a(t), -a(t) \mid ] \text{ for even } N \ (N \bmod 2 = 0),$$

$$\sigma - \text{mode: } \boldsymbol{X}(t) = [a(t), 0, -a(t) \mid a(t), 0, -a(t) \mid ...$$

$$... \mid a(t), 0, -a(t) \mid ] \text{ for } N \bmod 3 = 0,$$

$$\tau - \text{mode: } \boldsymbol{X}(t) = [a(t), 0, -a(t), 0 \mid a(t), 0, -a(t), 0 \mid ...$$

$$... \mid a(t), 0, -a(t), 0 \mid ] \text{ for } N \bmod 4 = 0. \qquad (7)$$

These modes correspond to the subgroups $G_2 = D_{N/2}$, $G_3 = D_{N/3}$ and $G_4 = D_{N/4}$ of the point group $G_0 = D_N$, respectively. The unit cells of the vibrational regimes (7) are larger 2, 3 and 4 times, respectively, than that of the equilibrium state ($l_0$). In other words, the *translational* symmetry of the original chain decreases by two, three or four times if we pass from the chain equilibrium state to its vibrational states corresponding to the $\pi$-, $\sigma$- or $\tau$-modes. Obviously, in the case of small amplitudes the above considered Rosenberg modes tend to the linear normal modes with wave vectors (wave numbers) $k = b/2$ ($\pi$-mode), $k = b/3$ ($\sigma$-mode), $k = b/4$ ($\tau$-mode), where $b$ is the period of the reciprocal lattice of the chain.

In dynamical simulations, above Rosenberg modes can be excited by the following initial conditions:

$$\pi - \text{mode: } \boldsymbol{X}(0) = [a, -a \mid a, -a \mid ... \mid a, -a],$$

$$\sigma - \text{mode: } \boldsymbol{X}(0) = [a, 0, -a \mid a, 0, -a \mid ...|a, 0, -a],$$

$$\tau - \text{mode: } \boldsymbol{X}(0) = [a, 0, -a, 0 \mid a, 0, -a, 0 \mid ...$$

$$... \mid a, 0, -a, 0],$$

where $a$ is an arbitrary value that determines the mode amplitudes, while the initial velocities of all particles of the chain are equal to zero $\dot{\boldsymbol{X}}(0) = [0, 0, 0, ..., 0]$. Note that $\pi$-, $\sigma$- and $\tau$-modes represent periodic dynamical regimes determined by only one parameter $a$.

The above presented displacement patterns (7) of $\pi$-, $\sigma$- and $\tau$-modes can be derived by demanding *invariance* of the general pattern $X(t)$ according to the groups $D_{N/2}$, $D_{N/3}$ and $D_{N/4}$ which are subgroups $G_j$ of the group $G_0 = D_N$ for the appropriate $N$. If we demand such invariance according to the group of *less* symmetry than the above listed subgroups $D_{N/2}$, $D_{N/3}$ and $D_{N/4}$

(for example, for $D_{N/5}$, $D_{N/6}$, etc.) the displacement pattern found from the condition $\hat{G}_j \boldsymbol{X} = \boldsymbol{X}$ will depend not only on *one* parameter $a$, but on two or more ($m > 1$) arbitrary parameters. As a result, we obtain in such a way (see details in [8]) dynamical object that determines *quasiperiodic* motion with m different basis frequencies of the Fourier spectrum. Such patterns can be expressed as a *superposition* of m different NNMs and they represent *bushes* of nonlinear normal modes [16, 17] with dimension $m > 1$. This is a reason why only three symmetry-determined Rosenberg NNMs can exist in monoatomic chains with arbitrary interatomic interactions.

Let us note that all types of symmetry-determined periodic and quasiperiodic vibrations in physical systems with discrete symmetries can be obtained with the aid of specific group-theoretical methods developed in the theory of *bushes* of nonlinear normal modes [16, 17]. The application of this theory to various mechanical systems can be found in [18–24].

Hereafter, we write $\pi$-, $\sigma$- and $\tau$-modes in the brief form

$$\pi - \text{mode: } \boldsymbol{X} = [a,\ -a],$$

$$\sigma - \text{mode: } \boldsymbol{X} = [a,\ 0,\ -a],$$

$$\tau - \text{mode: } \boldsymbol{X} = [a,\ 0,\ -a,\ 0],$$

pointing atomic displacements only in one unit cell of the vibrational state.

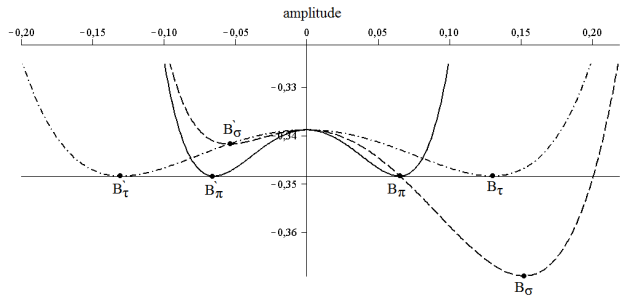


FIG. 16. Energy profiles of $\pi$-, $\sigma$- and $\tau$-modes for 15% strained carbon chain with $N = 12$ particles in the framework of the Lennard-Jones model.

## VI. PROPERTIES OF NONLINEAR NORMAL MODES IN THE FRAMEWORK OF THE LENNARD-JONES MODEL

It was shown in Sec.3 for the case of the $\pi$-mode that the L-J model allows one to describe dynamical and static properties of strained carbyne quite well. Let us consider applicability of this model for studying two other Rosenberg modes in the carbon chain with $N$ atoms. Below, we present detailed analysis for the case $N = 12$ because in such chain all three Rosenberg modes, $\pi$, $\sigma$ and $\tau$, can be exited by the appropriate initial conditions used in the computer simulations (periodic boundary conditions are assumed).

In Fig. 16, we depict potential energy profiles for $\pi$-, $\sigma$- and $\tau$-modes in the L-J chain strained by 15%. They are calculated for the "standard" Lennard-Jones potential, i.e. for the case where both phenomenological constants of the potential (4) are equal to unity ($A = B = 1$). All our results are given in the corresponding dimensionless units.

It is obvious from Fig. 16 that new equilibrium positions near the old one appear for all three Rosenberg modes. The points $B_\pi$, $B_\sigma$, $B_\tau$ correspond to $a > 0$, while $B'_\pi$, $B'_\sigma$, $B'_\tau$ correspond to $a < 0$. The profile of the $\sigma$-mode is asymmetrical according to the origin $a = 0$, while profiles of $\pi$- and $\tau$-modes are symmetrical and their minima are equal to each other. As a consequence, the equal height of potential barriers corresponds to $\pi$- and $\tau$-modes ($\Delta u_\pi = \Delta u_\tau = 0.005$). The height of the potential barrier of the $\sigma$-mode for the right well is equal to 0,015 that approximately thrice larger than that for $\pi$- and $\tau$-modes. The new equilibrium position ($a_{0\tau}$) for $\tau$-mode are twice more distant from the origin ($a = 0$) than that ($a_{0\pi}$) for the $\pi$-mode (see points $B_\tau$ and $B_\pi$ in Fig. 16).

We can explain the above properties of the potential profiles of the considered Rosenberg modes in the following manner.

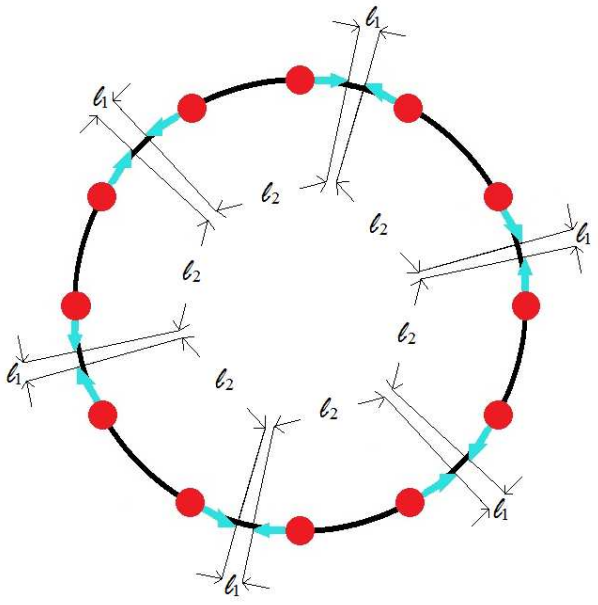


FIG. 17. Bond lengths alternation for the $\pi$-mode structure in the Lennard-Jones chain with $N = 12$ particles. Here $l_1 = l_0 - 2a$, $l_2 = l_0 + 2a$.

Let us consider Figs.17-19. We depict there L-J chains as rings of $N = 12$ particles for a fixed parameter $a$ (am-

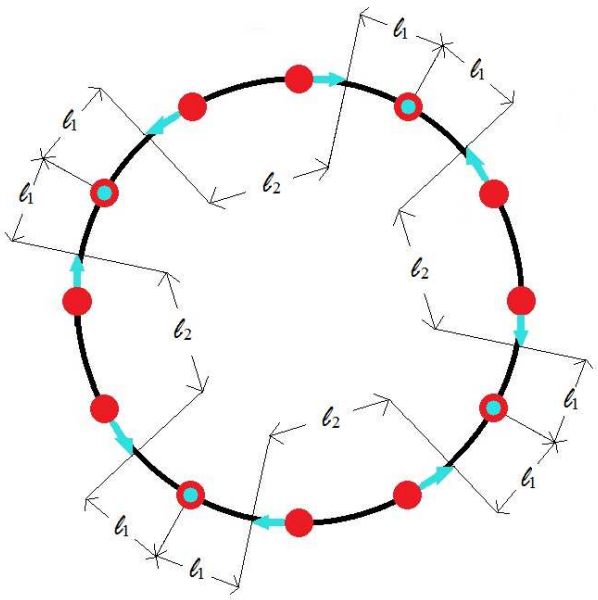


FIG. 18. Bond lengths alternation for the $\sigma$-mode structure in the Lennard-Jones chain with $N = 12$ particles. Here $l_1 = l_0 - a$, $l_2 = l_0 + 2a$.

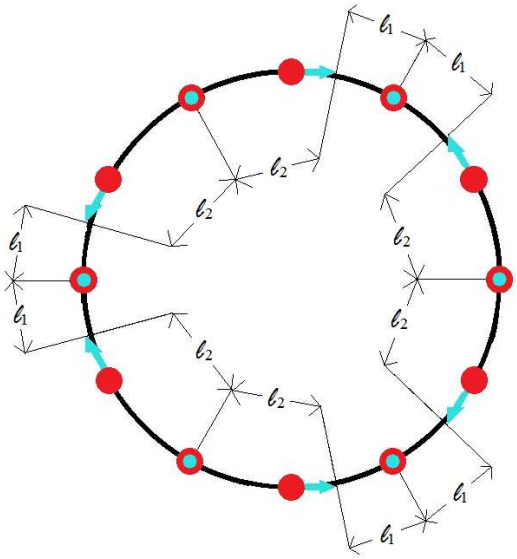


FIG. 19. Bond lengths alternation for the $\tau$-mode structure in the Lennard-Jones chain with $N = 12$ particles. Here $l_1 = l_0 - a$, $l_2 = l_0 + a$.

plitude) of $\pi$-, $\sigma$- and $\tau$-modes, respectively. The atomic displacements are shown by arrows. In each of these figures, one can see *two types* of interatomic distances (bond lengths), $l_1$ and $l_2$. For the $\pi$-mode, $l_1 = l_0 - 2a$ and $l_2 = l_0 + 2a$, where $l_0$ is the interatomic distance of equilibrium state of the strained chain. For $a > 0$, $l_1$ represents the short bond, while $l_2$ represents long one, and vice versa for $a < 0$. Thus the difference $\Delta l = |l_1 - l_2|$ between the interatomic distances turns out to be $\Delta l = 4|a|$. According to Fig. 17 the following sequence of the bond lengths (BLs) takes place for the $\pi$-mode:

$$BLA_\pi = [l_1 l_2 \mid l_1 l_2 \mid l_1 l_2 \mid l_1 l_2 \mid l_1 l_2 \mid l_1 l_2]. \qquad (8)$$

Let us consider a pair potential $\varphi(r)$, which describes interactions between neighboring particles placed at distance r from each other. There are six bond lengths (BLs) of $l_1$ type and six BLs of $l_2$ type in Eq. (8). Therefore, the whole potential energy $U(a)$ of the considered chain of $N = 12$ particles is equal to

$$U_\pi(a) = 6\varphi(l_1) + 6\varphi(l_2), \qquad (9)$$

where $l_1 = l_0 - 2a$, $l_2 = l_0 + 2a$. The position of the energy minima is determined by the equation

$$dU_\pi(a)/da = 0 \qquad (10)$$

from which we find

$$\varphi'(l_0 + 2a) = \varphi'(l_0 - 2a). \qquad (11)$$

If $x_0 > 0$ represents the root of the equation [3]

$$\varphi'(l_0 + x) = \varphi'(l_0 - x), \qquad (12)$$

then the new equilibrium position, corresponding to the bottom of the right potential well (point $B_\pi$ in Fig. 16) for the L-J chain with 15% strain, is equal to $a_0 = 0{,}075$ and, therefore, $\Delta l = 4a_0 = 0{,}30$.

Using the same method for the $\tau$-mode (Fig. 19) in the L-J chain, we obtain

$$l_1 = l_0 - a, \quad l_2 = l_0 + a, \quad \Delta l = 2a. \qquad (13)$$

$$BLA_\tau = [l_1 l_1 l_2 l_2 | l_1 l_1 l_2 l_2 | l_1 l_1 l_2 l_2], \qquad (14)$$

$$U_\tau(a) = 6\varphi(l_1) + 6\varphi(l_2), dU_\tau(a)/da = 0, \qquad (15)$$

$$\varphi'(l_0 + a) = \varphi'(l_0 - a). \qquad (16)$$

Therefore, $a_{0\tau} = x_0$ where $x_0$ is the root of Eq. 12. Comparing this result with that for the $\pi$-mode, $a_{0\pi} =$

[3] In Sec. III, we have solved this equation for the Lennard-Jones potential by simple graphic method.

$x_0/2$, we conclude that $a_{0\tau} = 2a_{0\pi}$, i.e. potential minimum for $\tau$-mode for *every* pair interparticle potential $\varphi(x)$ (not only for the Lennard-Jones potential!) is twice more distant from the origin at $a = 0$.

Let us now consider Fig. 18 corresponding to the $\sigma$-mode. We find from this figure for $a > 0$.

$$l_1 = l_0 - a, \quad l_2 = l_0 + 2a, \quad \Delta l = 3a, \tag{17}$$

$$BLA_\sigma = [l_1 l_1 l_2 | l_1 l_1 l_2 | l_1 l_1 l_2 | l_1 l_1 l_2], \tag{18}$$

$$U_\sigma(a) = 8\varphi(l_1) + 4\varphi(l_2). \tag{19}$$

Thus, equation $dU_\sigma(a)/da = 0$ for finding equilibrium position $a_{0\sigma}$ looks as follows

$$\varphi'(l_0 + 2a) = \varphi'(l_0 - a). \tag{20}$$

Note that this equation differs essentially from the Eqs. (11) and (16) for $\pi$- and $\tau$-modes. Indeed, both equations (11) and (16) are invariant under changing the sign of the parameter $a$. In contrast to that, Eq. (20) changes its form under the above transformation $(a) \to (-a)$ as follows:

$$\varphi'(l_0 - 2a) = \varphi'(l_0 + a). \tag{21}$$

Let us note that Eqs. (16) and (20) possess *different* roots. As a consequence, we obtain for the L-J model under 15% strain (see Fig. 16) $B_\sigma = 0{,}150$, while $B'\sigma = -0{,}075$.

The matter is that transformation $(a) \to (-a)$ changes the number of short and long interatomic distances (bond lengths), because $l_1 = l_0 - a$ is a short distance and $l_2 = l_0 + 2a$ is a long distance for $a > 0$, with the opposite situation for $a < 0$. For $N = 12$ particles chain, there are 8 short bonds and 4 long bonds for the case $a > 0$, while 4 short and 8 long bonds correspond to the case $a < 0$. This is the cause of the asymmetrical form of the potential profile of the $\sigma$-mode. (For the case of $\pi$- and $\tau$-modes the transformation $(a) \to (-a)$ remains the number of short and long bonds unchanged, they simply are transformed into each other $l_1 \leftrightarrow l_2$).

Thus, condensation of $\pi$-, $\sigma$- and $\tau$-modes results in different schemes of bond lengths alternation:

$$BLA_\pi = [l_1 l_2 | l_1 l_2 | l_1 l_2 | l_1 l_2 | l_1 l_2 | l_1 l_2], \tag{22}$$

$$BLA_\sigma = [l_1 l_1 l_2 | l_1 l_1 l_2 | l_1 l_1 l_2 | l_1 l_1 l_2], \tag{23}$$

$$BLA_\tau = [l_1 l_1 l_2 l_2 | l_1 l_1 l_2 l_2 | l_1 l_1 l_2 l_2]. \tag{24}$$

It seems to be plausible that there can exist two *new forms* of carbyne besides cumulene and polyyne. Indeed, all bonds are equal in cumulene $[l_1 l_1 l_1 ... l_1]$, while there are two different bonds in polyyne and in carbynes appearing as a result of condensation of $\sigma$- or $\tau$-modes, but they possess *different alternation schemes* as given by Eqs. (22) - (24).

The present experimental technique cannot allow one to find certainly the alternation of bond lengths in carbon chains. However, let us note that in [2] the rough attempt of finding bond lengths in strained carbon chain was realized by transmission electron microscope (TEM). One can hope that progress in the experimental technique will soon allow determining bond lengths alternation for strained carbyne with reasonable accuracy.

In conclusion, it is interesting to note that BLA depicted in Fig.1 of the paper [3], which was found by DFT simulations, is more close to the condensation of Rosenberg modes different from the $\pi$-mode, which corresponds to polyyne form of carbyne.

Now we consider the critical value $\eta_c$ of the strain for which old equilibrium positions of the carbon atoms in the chain with arbitrary pair potential $\varphi(r)$ lose their stability and new such positions appear. The potential energy $u(a)$ of the chain in the small vicinity of the parameter $a = 0$ has to possess minimum for $\eta < \eta_c$ and maximum for $\eta > \eta_c$.

Let us write, the first terms of the Taylor series of the function $u(a)$ near the point $a = 0$ for the $\pi$-mode [see Eq.(9)]:

$$u_\pi(a) = 6\varphi(l_0 - 2a) + 6\varphi(l_0 - 2a) = 12\varphi(l_0) +$$

$$+ 24a^2\varphi''(l_0) + ... \tag{25}$$

Obviously, maximum of the function $u_\pi(a)$ takes place if $\varphi''(l_0) < 0$ and minimum if $\varphi''(l_0) > 0$. Therefore, the critical value of the strain $\eta_c$ can be determined from the equation $\varphi''(l_0) = 0$, where $l_0 = l_0(\eta)$ is the interatomic distance of the chain in the equilibrium state under the strain $\eta$.

Thus, $\eta_c$ corresponds to the point at which curvature of the function $\varphi(r)$ changes sign. For the case of the Lennard-Jones potential $\varphi(r) = r^{-12} - r^{-6}$, we find that $\varphi''(r) = 0$ for $r = \sqrt[6]{\frac{26}{7}} \approx 1{,}244$, while equilibrium interatomic distance for the L-J chain without strain is equal to $r_0 = \sqrt[6]{2} \approx 1{,}122$. Therefore, $\eta_c = (r - r_0)/r_0\ 100\% \approx 10{,}87\%$.

Similarly to the above calculations, we obtain the following decompositions for the $\sigma$-mode and $\tau$-mode:

$u_\sigma(a) = 12\varphi(l_0) + 12a^2\varphi''(l_0) + ...$,

$u_\tau(a) = 12\varphi(l_0) + 6a^2\varphi''(l_0) + ...$

Therefore, we find *identical* conditions for obtaining the critical value $\eta_c$ for all three Rosenberg modes: $\varphi''(l_0) = 0$.

In other words, the stability bifurcation of the L-J chain with increasing of the strain $\eta$ takes place simultaneously for these modes, i.e. for the same $l_0$ corresponding to the point of zero curvature (inflection point) of the pair potential $\varphi(r)$. This point for the Lennard-Jones potential is shown in Fig. 20.

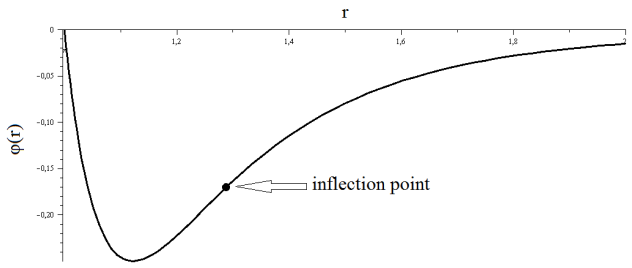


FIG. 20. The inflection point of the standard Lennard-Jones potential.

## VII. CONCLUSION

In this paper, we study properties of longitudinal nonlinear vibrations in strained carbon chains by ab initio methods, based on the density functional theory, as well as by the methods of molecular dynamics in the framework of the simple Lennard-Jones model, and also for arbitrary pair potential of the interparticle interactions.

In the brief paper [6], we have been reported that under sufficiently large uniform strain ($\eta > 11\%$) radical transformation of carbyne cumulene structure takes place as the result of condensation of the $\pi$-mode, which becomes a soft mode in a certain range of its amplitude. Indeed, in this case, the old equilibrium positions, around which carbon atoms vibrate in the case of small strain, lose their stability and two new such positions arise near each of them. This transformation corresponds to the Peierls phase transition in one-dimensional crystal and is associated with doubling of the unit cell. As a result, the carbyne chain transforms from the cumulene to polyyne form. This phase transition in strained carbyne chains was previously discovered in the work [1], which was also carried out by ab initio DFT simulations, but from another position compared to those of [6]. Indeed, we have studied nonlinear vibrations in carbyne chains, while the authors of [1] explored their static structure.

As was already emphasized in Introduction, the above phase transition is a phenomenon of great physical importance because it leads to a qualitative change in the electron spectrum of cumulene. Indeed, as a result of appearance of the energy gap in this spectrum, conductive cumulene transforms into polyyne which is semiconductor or insulator. In turn, it is expected that such change in electrical properties under mechanical strain can be used in some nanodevices.

In [1], a quantum-mechanical model of one particle moving in the double-well potential was introduced to explain the properties of the Peierls phase transition found in the framework of the DFT approach. Unlike this in [6], for the same purpose, a more simple classical model was introduced, which represents the chain of mass-points whose interactions are described by the Lennard-Jones potential (L-J chain). Using this model, we were able to explain not only the static properties, such as appearance of the new equilibrium positions, etc., but also the properties of nonlinear vibrations near these new equilibrium positions. Moreover, the approach developed in [6] allows us to consider the condensation of two other symmetry-determined Rosenberg nonlinear normal modes (besides the $\pi$-mode), which correspond to multiplication of vibrational unit cell three- or four times compared to that of cumulene equilibrium state. In turn, such approach leads to prediction of possibility for existence of two new forms of carbyne with the bond length alternations different from that of polyyne.

In dynamical regimes, described by Rosenberg modes, all particles of the system vibrate with the same frequency, but unlike the conventional linear normal modes, these vibrations are *nonlinear*. In [8], we proved with the aid of group-theoretical methods that in the monoatomic chains with arbitrary interactions only three Rosenberg modes, $\pi$, $\sigma$ and $\tau$, can exist. The unit cell of the vibrational states corresponding to $\pi$-, $\sigma$- and $\tau$-modes are two, three and four times larger than that of the chain equilibrium state.

The condensation of these modes induces the carbon structures with two different bond lengths and alternation schemes of these bonds are different for the structures induced by $\pi$-, $\sigma$- and $\tau$-modes [see Eqs. (22)-(24)]. The condensation of the $\pi$-mode generates the polyyne structure of the carbon chain, while condensation of $\sigma$- and $\tau$-modes may be associated with two new forms of carbon chains.

We use two different models to simulate dynamical and static properties of the above Rosenberg modes in strained carbon chains, the DFT model and the Lennard-Jones model. The former model is certainly more adequate because it takes into account the presence of electron shells near each carbon nucleus and provides quantum-mechanical approach for the electron subsystem. However, density functional theory cannot ensure exact consideration of the physical reality because of a number of approximations used in practical application of this theory. In this sense, the crucial role plays the choice of exchange-correlation functionals. It is known that such functional conventionally used in the software packages for DFT simulations (ABINIT, VASP etc.) cannot ensure acceptable approximation for calculation of van der Waals interactions [4] (see discussion of this prob-

[4] Note that the appropriate corrections to the exchange-correlation functionals are essentially *nonlocal*. As a consequence the LDA approximation and even GGA approximation cannot provide any satisfactory calculation of vdW interactions.

lem in [25–28]. On the other hand, the van der Waals (vdW) interactions turn out to be very essential for large strain of carbyne since the distances of its atoms are considerably greater than those in the chain without strain.

In the Lennard-Jones model, vdW interactions are taken into account by the last term of the potential (2), which is proportional to $r^{-6}$. Note that the main problem of the choice of vdW amendments to the exchange-correlation functionals is how to obtain their correct asymptotic ($r^{-6}$) [25–28].

We could not get an acceptable approximation in the framework of the DFT approach to simulate correctly the condensation of $\sigma$- and $\tau$-modes (obviously, the vdW interactions turn out to be more essential for these modes than for the $\pi$-mode[5]). As a consequence, our prediction of the possibility of existence of two new forms of carbon chains is based only on studying of the Lennard-Jones model.

Now let us return to consideration of stability properties of the new EQPs and of the periodic oscillations in their vicinity, which are discussed in Secs. III and IV of this paper. We present there computational experiments demonstrating that our Lennard-Jones model, which is rather accurate for prediction of new static and dynamical properties of the strained carbon chains, turns out to be unsatisfactory for analyzing stability of the new atomic equilibrium positions and stability of oscillations around them. Now we can indicate the following causes of such phenomenon.

As was already emphasized, the DFT model, unlike the L-J model, is more adequate in physical sense because it takes into account electron shells of each carbon atom, which adapt to any change in the nuclear configuration, while the L-J model deals with bare mass points. In other words, many degrees of freedom correspond to each site in the DFT model, while only one variable is associated with every site in the Lennard-Jones model. There is also a mathematical cause of the above discrepancy between DFT and L-J models. Indeed, in the case of the L-J model we study the stability of a solution of ordinary differential equations (classical Newton equations), while in the case of the DFT model one has to analyze the stability of the solution to a system of cumbersome integro-differential equations (Kohn-Sham quantum-mechanical equations).

Thus, the L-J model describes sufficiently well the *existence* of new equilibrium positions in strained carbyne, but it turns out to be unsatisfactory for analysis of their *stability*. We feel that such discrepancy between the results obtained by methods of molecular dynamics and those by DFT simulations may be typical for very different physical problems.

## ACKNOWLEDGMENTS

The authors are sincerely grateful to Profs. V. P. Sakhnenko, S. V. Dmitriev and N. V. Ter-Oganessian for useful discussions, and to I. P. Lobzenko for assistance in application of the software package ABINIT. This work was supported by the Russian Science Foundation.

[1] V.I. Artyukhov, M. Liu, and B.I. Yakobson, Nano Lett. **14**, 4224 (2014).
[2] G. Casillas, A. Mayoral, M. Liu, V.I. Artyukhov, A. Poncea, B.I. Yakobson, M.J. Yacaman, Carbon **66**, 436 (2014).
[3] M. Liu, V.I. Artyukhov, H. Lee, F. Xu, B.I. Yakobson, ACS Nano **7**, 10075 (2013).
[4] P.B. Sorokin, H.K. Lee, L.Yu. Antipina, A.K. Singh, B.I. Yakobson, Nano Lett. **11**, 2660 (2011).
[5] S. Cahangirov, M. Topsakal, S. Ciraci. Phys. Rev. B **82(19)**, 195444 (2010).
[6] G.M. Chechin, D.A. Sizintsev, O.A. Usoltsev, Letters on materials **6 (2)**, 146 (2016).
[7] W. Cochran, Phys. Rev. Lett. **3(9)**, 412 (1959).
[8] G.M. Chechin, D.S. Ryabov, K.G. Zhukov, Physica D **203**, 121(2005).
[9] W. Kohn. Rev. Mod. Phys. **71**, 1253 (1999).
[10] X. Gonze et al.Comput. Phys. Commun. **180**, 2582 (2009).
[11] www.abinit.org.
[12] D. W. Brenner. Phys. Rev. B **42**, 9458 (1990).
[13] A. Kistanov, E.A. Korznikova, S.Yu. Fomin, K. Zhou, S.V. Dmitriev, Letters on materials **4 (4)**, 315 (2014).
[14] R.M. Rosenberg, J. Appl. Mech. **29**, 7 (1962).
[15] A. F. Vakakis, L. I. Manevich, Y. V. Mikhlin et al., Normal Modes and Localization in Nonlinear Systems, Wiley, New York (1996).
[16] G.M. Chechin, V.P. Sakhnenko, Physica D **117**, 43 (1998).
[17] V.P. Sakhnenko, G.M. Chechin. Phys. Dokl. **38**, 219 (1993).
[18] G.M. Chechin, A.V. Gnezdilov, M. Yu. Zekhtser, Int. J. Nonlinear Mech. **38**, 1451 (2003).
[19] G. M. Chechin, K.G. Zhukov, Phys. Rev. E **73**, 036216 (2006).
[20] G.M. Chechin, D.S. Ryabov, Phys. Rev. E **69**, 036202 (2004).
[21] G.M. Chechin, S.A. Shcherbinin, Commun. Nonlinear Sci. Numer. Simulat. **22**, 244 (2015).
[22] G.M. Chechin, D.S. Ryabov, S.A. Shcherbinin, Phys. Rev. E **92**, 012907 (2015).
[23] G.S. Bezuglova, G.M. Chechin, P.P. Goncharov, Phys. Rev. E **84**, 036606 (2011).
[24] G.M. Chechin, D.S. Ryabov, S.A. Shcherbinin, Letters on materials **6**, 9 (2016).
[25] G. Roman-Perez, J.M. Soler, Phys. Rev. Lett. **103**, 096102 (2009).

[5] For example, the bottom of the potential well for $\sigma$-mode and $\tau$-mode are twice more distant from origin (see Fig. 15) than that of the $\pi$-mode.

[26] M. Dion, H. Rydberg, E. Schroder, D. C. Langreth, B. I. Lundqvist, Phys. Rev. Lett. **92**, 246401 (2004).
[27] Kyuho Lee, E.D. Murray, Lingzhu Kong, Bengt I. Lundqvist, David C. Langreth, Phys. Rev. B **82**, 081101 (2010).
[28] Kristian Berland, Per Hyldgaard, Phys. Rev. B **89**, 035412 (2014).